[27] Reference 26, p. 346.
[28] Niels Bohr and Fritz Kalckar, "On the transmutation of atomic nuclei by impact of material particles: I. General theoretical remarks," Kgl. Danske Vid. Selsk. Skr. **14**, 1–40 (1937).
[29] Reference 28, p. 12.
[30] Gregory Breit and Eugene Wigner, "Capture of slow neutrons," Phys. Rev. **49**, 519–531 (1936); see p. 519.
[31] Roger H. Stuewer, Ref. 25 p. 207.
[32] Hans A. Bethe and R. F. Bacher, "Nuclear physics A: Stationary states of nuclei," Rev. Mod. Phys. **8**, 82–229 (1936); Hans A. Bethe, "Nuclear physics B: Nuclear dynamics, theoretical," Rev. Mod. Phys. **9**, 69–244 (1937); M. Stanley Livingston and Hans A. Bethe, "Nuclear physics C: Nuclear dynamics, experimental," Rev. Mod. Phys. **9**, 245–390 (1937). Reprinted in *Basic Bethe. Seminal Articles on Nuclear Physics, 1936–1937* (Tomash Publishers and American Institute of Physics, New York, 1986).
[33] Roger H. Stuewer, Ref. 25, pp. 207–208.
[34] Otto Hahn and Fritz Strassmann, "Über den Nachweis und das Verhalten der bei der Bestrahlung des Urans mittels Neutronen entstehenden Erdalkali-metalle," Naturwiss. **27**, 11–15 (1939).
[35] Lise Meitner and Otto Frisch, "Disintegration of uranium by neutrons: A new type of nuclear reaction," Nature **143**, 239–240 (1939).
[36] For example, see Otto Frisch, *What Little I Remember* (Cambridge U.P., Cambridge, 1979); Otto Hahn, *Otto Hahn: A Scientific Autobiography* (Charles Scribner's and Sons, New York, 1966); Richard Rhodes, *The Making of the Atomic Bomb* (Simon and Schuster, New York, 1986); and Roger H. Stuewer, Ref. 25.
[37] Niels Bohr and John A. Wheeler, "The mechanism of nuclear fission," Phys. Rev. **56**, 426–450 (1939).
[38] Reference 23 (to be published).
[39] Reference 23 (to be published).
[40] N. H. Frank, "Note on the Hartree and Hartree–Fock methods," Phys. Rev. **51**, 577–583 (1937).
[41] George Gamow, *Structure of Atomic Nuclei and Nuclear Transformations* (Clarendon, Oxford, 1937), p. 52.
[42] Hans A. Bethe, Ref. 32 p. 174 (1937).
[43] Hans A. Bethe, Ref. 32 p. 179 (1937).
[44] Rudolf Peierls, Ref. 1, p. 195.
[45] Walter M. Elsasser, Private communication (1986).
[46] Emilio Segrè, in *Exploring the History of Nuclear Physics*, edited by Charles Weiner (American Institute of Physics, New York, 1972), p. 191.
[47] Victor Weisskopf, Ref. 46 p. 188.
[48] Eugene P. Wigner and Eugene Feenberg, "Symmetry properties of nuclear levels," Rep. Prog. Phys. **8**, 274–317 (1942); see page 275.
[49] H. A. Bethe and R. F. Bacher, Ref. 34, p. 150.
[50] G. Gamow, Ref. 44, p. vii.
[51] H. A. Bethe, "An attempt to calculate the number of energy levels of a heavy nucleus," Phys. Rev. **50**, 332–341 (1936).
[52] Reference 51, p. 338.
[53] M. E. Rose and H. A. Bethe, "Nuclear spins and magnetic moments in the Hartree model," Phys. Rev. **51**, 205–213 (1937).
[54] John Wheeler, Ref. 46, p. 44.
[55] H. A. Bethe, Ref. 46, p. 200.
[56] Victor Weisskopf, Ref. 46, p. 200.

The dynamical theory of the baseball bat

L. L. Van Zandt
Department of Physics, Purdue University, West Lafayette, Indiana 47907

(Received 14 February 1991; accepted July 1991)

A theory of the elastic behavior of an irregularly shaped, cylindrically symmetric object is developed and applied to the study of the familiar baseball bat. The normal mode, standing wave patterns of elastic vibrations are obtained and displayed graphically. The lowest 20 normal modes, extending in frequency up to about 3 kHz, are used to study and display the elastic response of the bat in the first few milliseconds after striking a ball. The contribution of the normal mode elastic vibrations to the hit ball speed is also developed, and the consequences for the batter (and fielders) are explored.

I. INTRODUCTION

Without widespread interest in the game, the physics of the baseball bat would be considerably less interesting. Because of the game, however, almost all American readers have knowledge of this curious cultural artifact as well as working experience in its use. This lends importance to what might otherwise be a matter of limited application and interest.

The baseball bat can serve as a familiar medium to draw the attention of students and lay audiences to the general subject of vibrations and waves, the dynamics of collisions, the flight of projectiles, the theory of elastic deformations, and a few other related subjects. As we see in the following, all these topics are prominently involved in developing a theory of the bat. It is appropriate that there is already a significant literature dealing with the behavior of this wooden cudgel.

The bat is a homogeneous, elastic bar of varying cross section. The regulations specify no more than a maximum diameter ($2\frac{3}{4}$ in.) and a maximum length (42 in.), leaving considerable room for adjustment of the shape. As it develops, the longitudinal contours have interesting consequences in the dynamical behavior, and possibly in the game as well. The irregular shape also precludes any possibility of accurate analytical solution for a realistic model. It is clear from the outset that the tool for study of the bat is the computer.

In the following sections, we will first develop a set of equations describing the motion of the bat as an elastic object. We then use these equations to find the normal modes of vibration, that is, the standing wave forms the bat can support and their characteristic frequencies. Some recent experiments on the vibration of a bat by Brody[1] are discussed in light of these normal modes.

Following this, we can develop the effect of the various bat vibrations on the recoil of the ball. There are some mild surprises in this latter result with possibly some consequences for the game. We verify what every pitcher knows—that the outside edges of the plate are dangerous territory for the defense—and add some new reasons why this should be true.

Finally, we display the effect of the ball impact on the bat motions. These prove to be complex, but overall sustain the customary assertions about the "sting" of the bat, the handle motion resulting from an improperly hit ball.

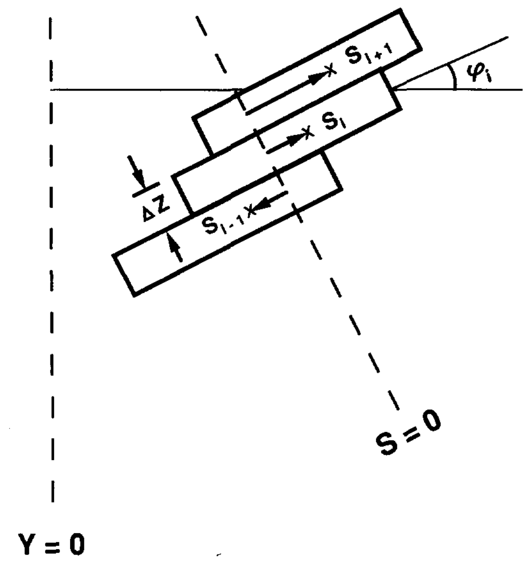

Fig. 1. The sliced loaf model of a bending beam. Three slices of an arbitrary bent and sheared bar are shown sheared relative to each other. Slice i is displaced from the axis of the beam by a distance S_i. The axis of the beam, at this point, makes an angle of φ_i with respect to the equilibrium longitudinal direction.

II. THE MODEL AND EQUATIONS OF MOTION

The wave equation for compressional waves on a uniform, homogeneous bar can be found in standard references such as Morse' "Vibration and Sound."[2] This conventional approach is unsatisfactory for a study of the bat in several respects. Most conspicuously, the bat is not uniform in cross section. There is no analytic approach that will be successful for arbitrary contours such as those we wish to study. Second, the conventional theory of beam deformation assumes at the outset that the deformations are locally of pure longitudinal compressional character. The method we develop here shows that while this is a good approximation at the lowest few frequencies, there is a shearing component to the motions. This shearing does not change the qualitative behavior of the modes, but does alter the numerics in a measurable amount. A final difficulty is that the no-shear "simplification" leads—for the uniform bar—to a fourth-order equation in the bending derivatives. When this formalism is extended to the nonuniform case of the bat, the resulting numerical system is outside the capabilities of most numerical packages, producing a so-called polynomial eigenvalue equation to be solved. The method we develop here, by contrast yields a pair of coupled second-order equations. In mathematical principle these are of the same level of complication, but in execution on the computer, our system proves a much more tractable problem.

We imagine the bat sliced up like a loaf of bread, i.e., composed of a number of parallel, circular sections elastically coupled to their neighbors. Each section is capable of transverse displacement and rotation about a transverse axis. We consider only the case of a directly hit ball, thereby obviating the need to treat any torsional motion of the bat. We also do not include any transverse compression of the individual slices in the motion.

In Fig. 1 we show three neighboring slices undergoing displacement and subsequent motion. The force between neighbors arises from their relatively sheared displacements and their relative rotations. In Fig. 1, however, we show only relative shearing displacements; slices i and $i+1$ are sheared by a distance

$$\Delta s = s_{i+1} - s_i .$$

The S_i are measured perpendicular to the local central axis direction. The centers of the slices are separated by a distance Δz along the longitudinal axis. From the elementary definition of the shear modulus, slice i experiences a transverse force along its upper face equal to

$$F_i = SA_i (s_{i+1} - s_i)/\Delta z. \tag{1a}$$

A_i is the upper face contact area of the two slices. A similar force acts on the lower face in the opposite direction:

$$F_{i-1} = SA_{i-1} (s_{i-1} - s_i)/\Delta z. \tag{1b}$$

The coordinates s_i are measured transversely with respect to the neutral axis of the bar. This axis may be displaced from the equilibrium position and orientation by shear and bend in earlier sections of the beam. It is important to measure displacements in an intertial system before invoking Newton's second law. Hence, we write

$$y_{i+1} - y_i = s_{i+1} - s_i - \varphi_i \Delta z. \tag{2}$$

As indicated, φ_i is the angle between the plane of the ith slice and the equilibrium z direction. We can combine these three equations to find the net transverse translational force on a slice and set this equal to its mass $\times$ acceleration:

$$m_i \ddot{y}_i = (S/\Delta z)[A_i(y_{i+1} - y_i + \varphi_i \Delta z) - A_{i-1}(y_i - y_{i-1} + \varphi_{i-1}\Delta z)]$$

or

$$m_i \ddot{y}_i = (S/\Delta z)[A_i(y_{i+1} + y_{i-1} - 2y_i + (\varphi_i - \varphi_{i-1})\Delta z) + (A_i - A_{i-1})(y_i - y_{i-1} + \varphi_{i-1}\Delta z)]. \tag{3}$$

Figure 2 shows the same three neighboring slices, but

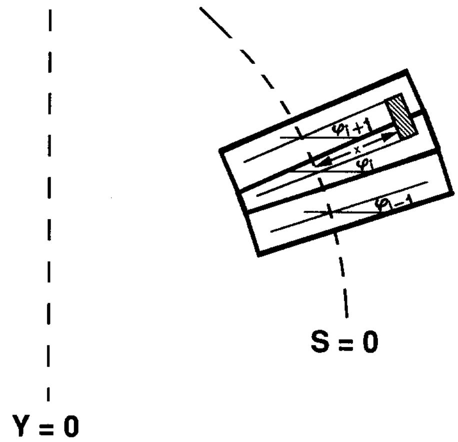

Fig. 2. The sliced loaf model of a bending beam. Three slices of an arbitrary bent and sheared bar are shown rotated relative to one another, resulting in a bend in the beam in this region. Slice i makes an angle of φ_i with the equilibrium direction of the beam axis. φ_i is the accumulated result of all φ_j, $i>j$. A small bar of cross-sectional area $dx\,dy$ and length Δz oriented along the longitudinal and located at a distance x from the neutral axis is shown. Because of the bending, this little bar is under compressional stress.

this time they are not sheared, but rotated with respect to one another producing a bending of the bar. Partway out from the neutral axis a distance x, we also show a little section of the beam whose dimensions are dx, dy, $l = \Delta z$. As drawn here, this little bar is subject to length strain in the amount

$$\Delta l = x(\varphi_{i+1} - \varphi_i).$$

It therefore exerts longitudinal forces on the i and $i+1$ slices:

$$\delta f = (\Delta l / l) Y\, dx\, dy. \tag{4}$$

The net translational force exerted by all such little bars on the two slices is zero because of the antisymmetry between the left and right sides of the neutral axis. The net torque on the slices does not vanish:

$$\delta\tau = (Yx^2/\Delta z)(\varphi_{i+1} - \varphi_i)\, dx\, dy. \tag{5}$$

Over the total surface of the slice, this integrates to a torque of

$$\tau = (Y\pi R_1^4 / 4\Delta z)(\varphi_{i+1} - \varphi_i). \tag{6}$$

The net torque on a slice from slices above and below is found by adding two such torques:

$$\tau_i = (Y/4\Delta z)\left[A_i R_i^2(\varphi_{i+1} + \varphi_{i-1} - 2\varphi_i) + (A_i R_i^2 - A_{i-1} R_{i-1}^2)(\varphi_i - \varphi_{i-1})\right]. \tag{7}$$

There is an additional torque acting on a slice. Referring again to Fig. 1, note that the shearing force on the upper face of the slab exerts a clockwise rotational effort. The moment arm of this, with respect to the slab center of mass, is $\Delta z/2$. A similar torque, in the same sense, is exerted by the shearing force from the lower slice. Combining these two torques gives

$$\tau_S = -S\{A_i[y_{i+1} - y_{i-1} + (\varphi_i + \varphi_{i-1})\Delta z] - (A_i - A_{i-1})(y_i - y_{i-1} + \varphi_{i-1}\Delta z)\}. \tag{8}$$

We combine the torques and set the result equal to the product of slice moment of inertia about the y axis and the angular acceleration. Defining $\Phi_i = \varphi_i \Delta z$ and recapitulating, we have two coupled sets of equations of motion:

$$\ddot{y}_i = \frac{S}{\rho\Delta z^2}\left(y_{i+1} + y_{i-1} - 2y_i + \frac{\Delta A_i}{A_i}(y_i - y_{i-1})\right) + \frac{S}{\rho\Delta z^2}(\Phi_i - \Phi_{i-1}), \tag{9a}$$

$$\ddot{\Phi}_i = \frac{Y}{\rho\Delta z^2}\left(\Phi_{i+1} + \Phi_{i-1} - 2\Phi_i + \frac{\Delta(A_i R_i^2)}{A_i R_i^2}(\Phi_i - \Phi_{i-1})\right) - \frac{2S}{\rho R_i^2}\left[(y_{i+1} - y_i + \Phi_i) + \left(1 - \frac{\Delta A_i}{A_i}\right)(y_{i+1} - y_i + \Phi_i)\right]. \tag{9b}$$

These two equations, together with appropriate boundary conditions, describe the complete dynamics of the baseball bat. In the limit of very many, very thin slices, these equations contain certain obvious combinations like $y_{i+1} + y_{i-1} - 2y_i$ that go over into second derivatives with respect to position z. There are also, manifestly, several first derivative terms, particularly in connection with the changing diameter of a beam of arbitrary contour.

We use the boundary condition that the shearing force and the torque on the endmost slices comes only from the next inner slice, otherwise taking the forms we have given above. That is to say, we treat the bat as a free object during the moments of its dynamics that we study. Brody[1] has pointed out, based on his measurements, that this assumption seems appropriate. It is certainly correct for the larger, club end of the bat. We will see, however, in the following, that the results of interest are essentially independent of the boundary condition at the handle end. Thus the assumption of free end boundary conditions is no approximation at all.

III. THE NORMAL MODES

The free vibrations of an elastic system are its normal modes. Without external driving forces or clamps at the ends, they are found from Eqs. (9a) and (9b) by assuming a single frequency for the motion and hunting for solutions of the resulting eigenvalue/eigenvector problem. Assuming an angular frequency ω, we have

$$\ddot{y}_i = -\omega^2 y_i \tag{10}$$

and a similar relation for the Φ_i's. If we think of all the y_i and the Φ_i stacked into one tall eigenvector Ψ we can express Eqs. (9) in the compact form

$$H\Psi = -\omega^2\Psi, \tag{11}$$

H, the "Hamiltonian" in this Heisenbergish looking equation is the matrix of coefficients taken from Eq. (9) above. The rank of the problem is $2N$, where N is the number of slices into which the bat is imagined to be separated. Because the bat is actually a continuum for all practical purposes, the number of slices must be large enough that each wavelength of the solution states encompases many slices. In what follows, N was chosen to be 75. The length of the bat was 0.864 m, so each slice was a little larger than 1 cm. This means the results grow less trustworthy as the mode wavelengths fall below 5 or 10 cm. This condition is well satisfied in our calculation since the Fourier analysis is nicely convergent, and the shorter modes contribute less to the final results. We terminate the series at mode #20 (19/2 wavelengths), for which one wavelength comprises eight slices.

Although all important contributions to the elastic behavior of the bat under ball impact conditions are satisfied by the first 20 normal modes, it proves not to be the case that everything of interest is exhausted by the first nontrivial mode as is sometimes asserted. In fact, the higher modes make a significant and surprising contribution to the flight of the ball.

The diagonalization of a matrix H like the one to which we have been led, is a routine matter for most computer systems. The Purdue Physics Department Computer "Gibbs," having approximately the capabilities of a VAX 780 contains the EISPACK series of routines in its FORTRAN library. Similar matrix manipulating routines are also available from IMSL (Houston, TX), and most medium sized scientific facilities have such a library on line.

A wooden bat was borrowed from my son's collection and calipered at a series of equally spaced points along its length. It was also weighed. It was comfortably within the specifications for major league play; as described above, these are none too restrictive. The length was 0.864 m, the mass 0.921 kg, the moment of inertia 0.0433 kg m^2. The material is apparently ash, the wood of choice for modern bats. (Hickory was popular a few decades ago.) This bat was manufactured by H&B Co. of Louisville, KY and bears a model number BB296.

The mechanical properties of many woods have been measured. The value for Young's modulus of ash was obtained from the Purdue Forestry Department, $Y = 1.20 \times 10^{10}$ N/m^2. The value for the shear modulus is less reliably known. We used $S = 8.8 \times 10^8$ N/m^2. Fortunately, the shear modulus affects the results much less than does the compressive modulus, so its uncertainty is less important. (If the moduli are regarded as adjustable parameters, essentially perfect agreement with experiment is possible. See Sec. VIII.)

A "computer" bat of invented cross sections was also treated. This imaginary bat had a somewhat thinner handle and a more abrupt conical section tapering up to the club portion than did the real bat. This imaginary bat differed in no important way from the real one in its dynamics. It served to point up the frequency sensitivity of the modes to handle contour.

Table I gives the first 20 eigenfrequencies of the real bat. The frequencies of the two lowest modes are zero. These correspond to simple transverse displacement, and to free rotation. For the case studied, that of the free bat, there are no restoring forces against this motion, hence the frequencies must vanish. The first nontrivial mode is #3, with a frequency of 136.8 Hz. Brody[1] reports a frequency of 27 Hz for the lowest mode of a clamped softball bat, otherwise undescribed. He also finds an unclamped mode at 163 Hz. Brody attributes this 163-Hz measurement to the simple bending mode; since we are dealing with different bats, there may be no conflict here. Brody's is a softball bat, suggesting a proportionally thinner club and thicker handle than our baseball bat. (In fact, the agreement can be made even better. See Sec. VIII.)

In Fig. 3 we display graphically the eigenvectors of the first five nontrivial modes. (The transverse displacements have been much exaggerated, relative to bat dimensions.) The lowest, at 137 Hz, is the simple bend. If clamped near the handle, this mode would go down in frequency, owing to the much greater mass to swing about a correspondingly longer moment arm. As we go up in frequency, the number of nodes increases by one at each step. The oscillations tend to be crammed into the weaker, handle portion of the bat, but as we look at the higher modes, we see notable deformation of the thick club portion.

This series of normal modes is entirely analogous to the harmonics of a stretched string or an organ pipe treated in introductory physics books. Here, however, the overtones are far from harmonic, and there are no symmetries or regularities.

It is clear why the lowest frequencies are so sensitive to the details of the cross-section contour. The bending strength of a beam varies as the 4th power of the cross section, and this is immediately reflected in a first power dependence of the frequency.[2] Furthermore, the tapering section bounds the weak, flexible handle, effectively defining the wavelengths. Hence, all the lower frequencies could be "tuned" by adjusting the handle thickness and taper slightly. In this paper, we do not offer any reasons for doing such a tuning. However, were one motivated to tune the modes, it would certainly be much less consuming of time and lumber to do this tuning on the computer, at least initially.

Table I. Frequencies of the first 20 normal modes.

Mode No.	Frequency in Hz
1	0.0
2	0.0
3	136.8
4	465.7
5	921.4
6	1464.2
7	2068.4
8	2713.6
9	3383.4
10	4064.5
11	4753.3
12	5433.1
13	6109.9
14	6784.6
15	7446.6
16	8097.4
17	8736.0
18	9351.5
19	9936.7
20	10480.3

IV. THE RESPONSE OF THE BAT

The calculation of the normal mode properties is an interesting and amusing exercise. In this section, however,

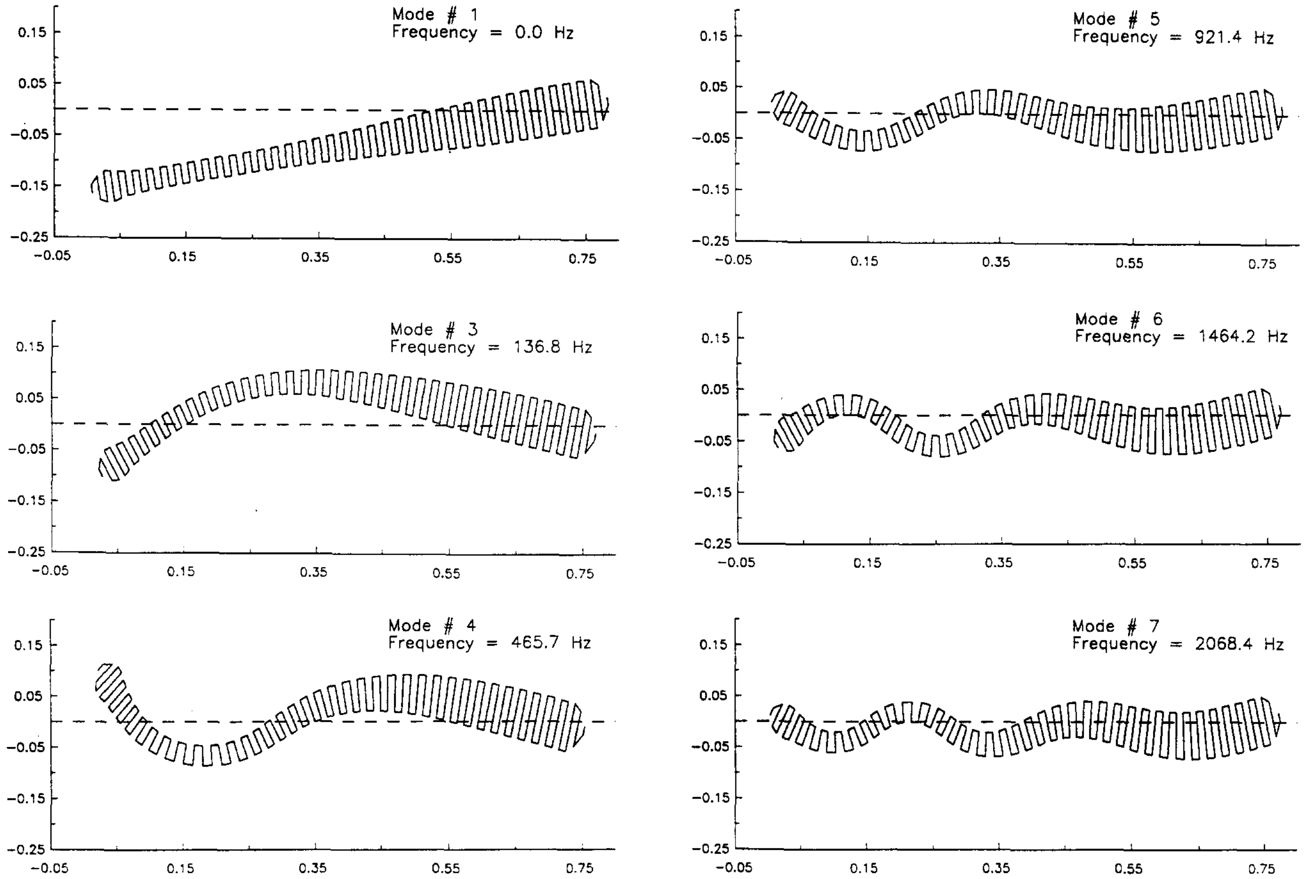

Fig. 3. The normal modes of a baseball bat. Seven of the lowest frequency, longest wavelength normal mode, standing wave patterns of an elastic bat are shown. The waves have been given a high amplitude relative to the transverse dimensions of the bat in order to emphasize their shapes in the figure. Each figure shows 75 slices displaced and rotated according to the eigenvector components y_i and φ_i computed from the normal mode analysis. Modes #1 and #2 (not shown) are simple uniform transverse displacement and simple rotation in an arbitrary mixture. Mode #3 is a simple bending; it has two nodal points, $y = 0$. Mode #7 has six nodes.

we make use of these modes and show how they can be used to determine the actual dynamics of impact between ball and bat. To do this, it is necessary to model the impact process. The idea is to be able to say how much of each mode is excited by the ball impact. Then adding the effects of all the modes, we find the behavior of the bat at any time and any point.

The duration of the impact is known to be about 1.5 ms.[3] We have assumed a parabolic shape in time for the interaction force:

$$f_c = p_0(6/\tau^3)(\tau - t)t \tag{12}$$

(and zero for $t<0$ or $t>\tau$).

The form is normalized to p_0, so that

$$\int f_c(t)dt = p_0.$$

We will later set p_0 equal to the momentum change of the hit ball.

We also spread the contact force out along the bat length, similarly modeling it with a parabola. We assume

$$f_i = \frac{(3 - i + i_0)(3 + i_0 - i)}{35} f_c \tag{13}$$

(zero, of course, where this expression would be negative). This spreads out the impact over five of the slices, weakly toward the edges, maximally at the central slice i_0. Spreading the impact is without effect on the lowest modes, but tends to reduce the importance of the higher ones by partially integrating over a greater fraction of their wavelength. The 35 in the denominator maintains the normalization of the hit to the total impulse transmitted to the ball p_0.

We now have an external force on each slice to add into the equations of motion. Also, since these equations in their final form, Eq. (9), were divided by the mass of each slice i, the force terms f_i need also to be divided by $\rho A_i \Delta z$, the mass of a slice.

We express the complete bat motion as a sum over normal modes:

$$\Psi = \sum_q A_q(t)\Psi_q. \tag{14}$$

We can do this because the normal mode solutions are orthogonal and complete in the spatial coordinate. Now we write the equations of motion for the time variation.

$$\ddot{\Psi}_i = \sum_q \ddot{A}_q \Psi_{qi} = H_{ij}\Psi_j + \frac{f_i}{m_i}$$

$$= \sum_q A_q H_{ij} \Psi_{qj} + \frac{f_i}{m_i}. \tag{15}$$

Now using Eq. (11) we can write more compactly

$$\sum_q \ddot{A}_q \Psi_{qi} = -\sum_q \omega_q^2 A_q \Psi_{qi} + \frac{f_i}{m_i}, \tag{16}$$

then multiply by Ψ_{Qi} and sum over i to obtain

$$\ddot{A}_Q = -\omega_Q^2 A_Q + f_Q, \tag{17}$$

where

$$f_Q = \sum_i \frac{\Psi_{Qi} f_i}{m_i} \left(\sum_i \Psi_{Qi}^2 \right)^{-1}. \tag{18}$$

It is easy to verify by direct differentiation that

$$A_q(t) = -\frac{1}{\omega_q} \int_{-\infty}^{t} \sin(t-t') f_q(t') dt'. \tag{19}$$

This form is valid even during the impact process, but performing the general integration produces a somewhat untidy collection of trigonometric functions. In what follows, we will mostly confine our attention to times equal to or later than the complete impact. Hence, we can replace the integration with the definite integral:

$$\begin{aligned} A_q(t) = &-f_q(1/\omega_q^4) \\ &\times [\sin \omega_q t(\omega_q \tau \cos \omega_q \tau + \omega_q \tau - 2 \sin \omega_q \tau) \\ &- \cos \omega_q t(\omega_q \tau \sin \omega_q \tau - 2 + 2 \cos \omega_q \tau)]. \end{aligned} \tag{20}$$

In this expression, f_q is $f_Q(t)$ with the factor $t(t-\tau)$ removed.

In the final expressions, we have included one further time dependence. We have given an exponential damping factor to each mode. The source of this damping is the internal friction, the intrinsic dissipation of the wood itself. We have very little data to use for the assignment of damping parameters, but Brody's oscilloscope traces suggest a "Q" of about 10. Hence, we have multiplied each $A_q(t)$ by an additional factor of $e^{-\omega_q t/10}$. This damping is independent of and additional to that coming from the batter's hands. As we see below, this is a small but significant matter in the flight of the ball. It also bears on the question of the differences between wooden and aluminum bats.

V. THE STING OF THE BAT

Now that we know the Ψ_q from the normal mode calculation and $A_q(t)$ from the time equation, we can use Eq. (14) to find the behavior of any of the slices at any time. As an illustration, Fig. 4 is a portfolio of figures showing the bat at a sequence of times following impact. As in the normal mode display, the displacement amplitudes have been exaggerated for graphic purposes. At $t = 0.0005$ s, we see the bat still in contact with the ball. By $t = 0.0015$ s the ball has just completed contact. We are viewing the bat in its own rest frame; there is neither rotation nor translation in these views. A deformation travels away from the impact point at 0.65 m. The center of percussion lies at 0.68 m and the node of the first deformation wave, mode 3, lies quite close at 0.69 m. (The conjugate point to the COP was taken as 10 cm, approximately in between the hands.)

Note that the handle has not yet moved. The flight of the ball is already completely determined, but the handle is undisturbed. Hence, our assertion above that the ball dynamics are independent of the boundary conditions on the elastic modes at the handle.

In subsequent milliseconds, we see the disturbance propagate from the stiff, thick portion into the thinner, more compliant portion of the bat. It is evident, without even checking the numerical values of the A_q, that several more modes above the simple bending of mode #3 are strongly involved in the motion. As the impulse passes into the handle, its amplitude grows, and the handle whips *forward*. A right-handed batter will feel the initial slap on his left palm and right fingers, at about 2.5 ms after the hit.

This motion also explains another oddity, well known to baseball hitters: when a bat breaks in play, it splinters on the catcher's side. Insight unguided by our analysis would suggest that upon impact the bat bends in the hitter's hands away from the pitcher to produce splintering on the pitcher's side. Clearly, however, when struck inside of the node, as in this example, the bat will bend concave to the pitcher. Professional pitchers are well aware that inside pitches yield broken bats.

We continue watching the motion, and see the handle come back at between 4 and 5 ms to slap the opposite hand and fingers. In an actual hit, the hands absorb this energy, and the bat motion becomes additionally damped.

Figure 5 shows a set of images in which the ball has struck at the "sweet spot," in this case just past the node of the mode #3 vibration, located at 0.69 m. As we would have imagined, the amplitude of the handle vibration is greatly reduced. Also shown in Fig. 5 are images of the bat struck an equal distance to the distal side of the node. Here we see the initial handle swing is back toward the catcher and smaller in amplitude.

VI. THE FLIGHT OF THE BALL

We can also use our knowledge of the $A_q(t)$ to study the flight of the ball and how it may be influenced by the vibrations. In this we find some interesting surprises.

In what follows, we have assumed a ball pitched at 40 m/s = 89 mph. The batter swings, producing a center of mass velocity of 16 m/s and an angular velocity of 34 rad/s, approximately equivalent to the bat pivoting around the handle at the instant of impact. These parameters are comfortably within the range of professional performance, but outside the capabilities of most little leagures or amateurs at a picnic.

The theory of ball recoil involves three conditions: (1) conservation of momentum, (2) conservation of angular momentum, and (3) the coefficient of restitution. The first two are straightforward; the third requires some discussion.

If the mass of the ball is m, and the mass of the bat is M, and the prehit ball velocity is v_1 and the prehit center of mass bat velocity is u, then the momentum condition gives

$$mv_1 + Mu = mv' + Mu'; \tag{21}$$

v' is the speed with which the hit leaves the plate, u' is the final bat speed. Of course, v_1 will be negative.

The bat will have an angular velocity Ω leading to an angular momentum $I_{\text{com}}\Omega$ about the bat center of mass. Likewise, the ball has initial angular momentum $mv_1 r_1$; r_1 is the impact point measured from the center of mass at R. Thus the second condition

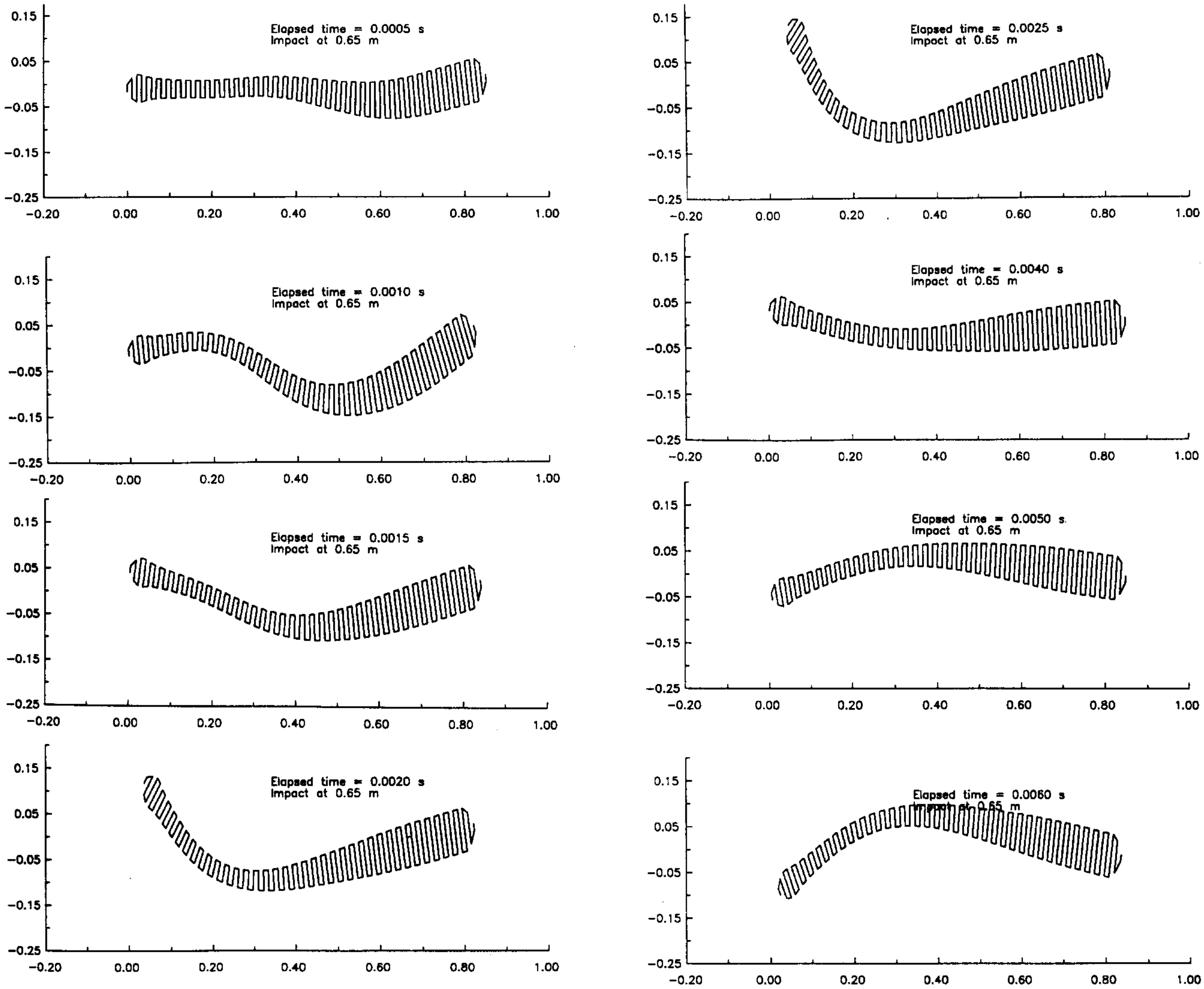

Fig. 4. The elastic response of the bat after striking the ball. Struck 4-cm proximally to the #3 vibration node, the bat undergoes a complex pattern of bends propagating from the impact point into the handle, eventually settling down to a #3 mode vibration after 4–5 ms. In these figures, the impact point was on the top of the bat. In the first two images, the amplitude was exaggerated an additional 2.5 X.

$$mr_1 v_1 + I\Omega = mr_1 v' + I\Omega'. \tag{22}$$

The coefficient of restitution is defined as the (negative) ratio of relative speeds of two objects after and before collision. It is a convenient quantity to work with because, unlike the kinetic energy, it does not depend on the choice of coordinate frames. The ball/bat collision is a complex event in which a severely deformed ball dissipates a substantial fraction of its energy among the woolen threads in its interior. Major league specifications call for a coefficient of restitution of 54.6 ± 3.2% for an 80-mph collision with a wooden barrier. The game itself is very hard on the ball, and they are changed frequently as the COR degrades. (A summer's play in the major leagues, about 2000 games, requires well upwards of 100 000 baseballs.)

The relative speed before collision is

$$s_i = (u + r_1 \Omega) - v_1. \tag{23}$$

After colliding, the relative speed is

$$s_f = (u' + r_1 \Omega' + v_{\text{elas}}) - v'. \tag{24}$$

The quantity v_{elas} is the speed of the bat surface in the bat rest frame arising out of its elastic response to the hit; it is the time derivative of the displacements we computed in the description above of Figs. 4 and 5.

We use Eqs. (23) and (24) together with the official COR value to obtain a third equation on the various speeds u', v', and Ω' characterizing the system motion after collision. To find v_{elas} we use our knowledge of the $A_q(t)$—actually their time derivatives taken from Eq. (20)—evaluated at $t = 0.0015$ s. We sum over the first 20 normal modes having amplitudes $A_q(t)$ to find y_{i_0} and its velocity as the collision ends.

The quantity p_0 in the expression for the interaction force, Eq. (12), is set equal to the change in ball momentum:

$$p_0 = m(v_1 - v'). \tag{25}$$

The system of equations can be readily solved for the final ball speed v' as a function of the point of impact along the bat (and the various initial parameters):

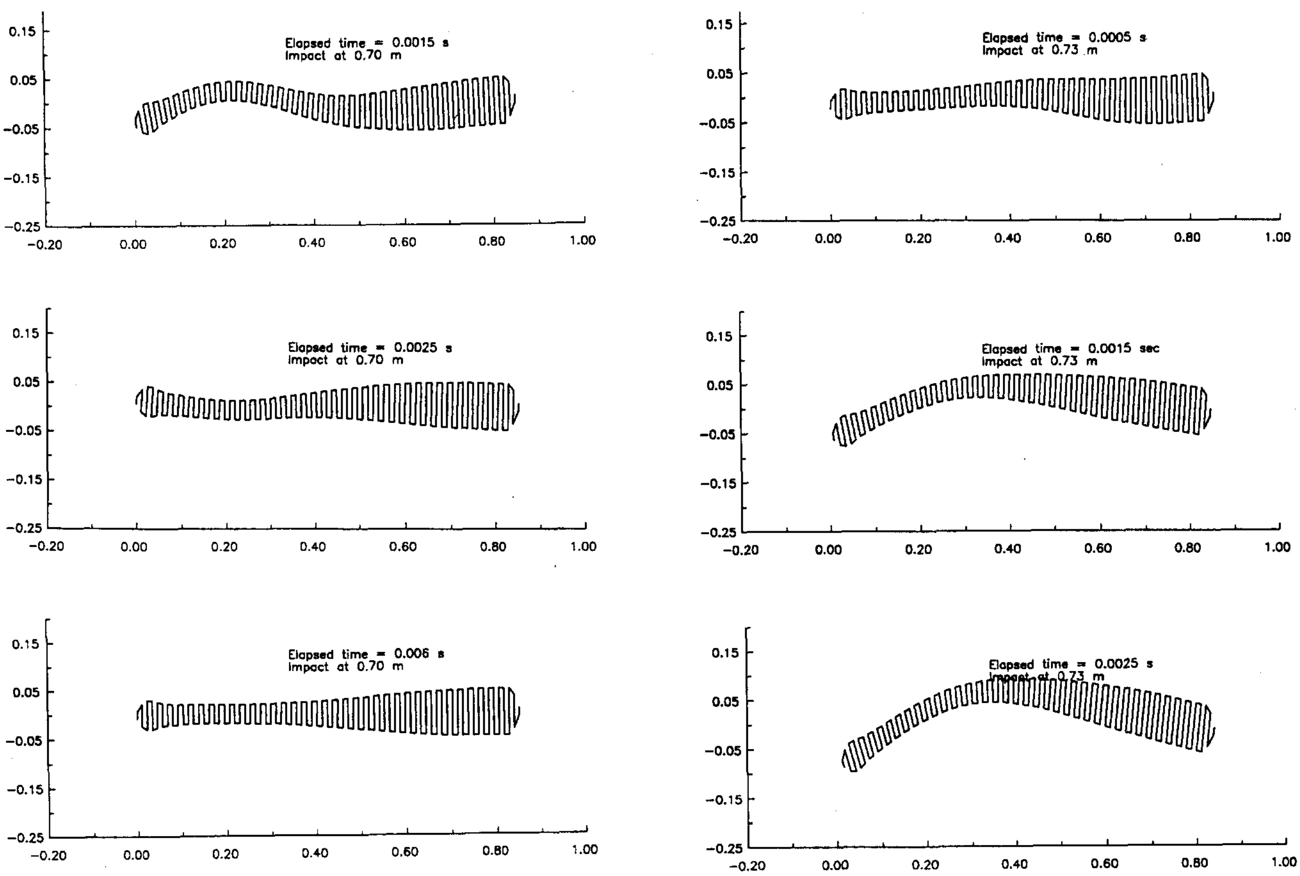

Fig. 5. Views of the elastic bat 1.5, 2.5, and 6 ms after impact with a ball at the node of mode #3. The times were chosen to coincide with the maxima of the handle distortions appearing in Fig. 4. The absence of mode #3 has greatly reduced the motion of the handle. This result, well understood by every child on the playground, provides one definition of the "sweet spot." Three more figures show the bat configuration for a bat striking the ball 4 cm distally to the #3 mode "sweet spot." The phase of the bending motion is reversed, relative to Fig. 4, and the ultimate handle motion somewhat reduced in amplitude.

$$v' = \frac{MI(1+e)u + (m - Me - amM)Iv_1 + MI\Omega(1+e)r_1 + Mmv_1r_1^2}{I(m + M - mMa) + Mmr_1^2}. \qquad (26)$$

In this equation, we have dropped the com subscript from I_{com}, and a is bat surface velocity divided by p_0, i.e., v_{elas} per unit impulse.

Besides simply plotting this equation, one of the very interesting things to do is consider the several contributions to a. Figure 6 shows the recoil speed of the ball as a function of impact point along the bat for three different cases. The starred curve sets $a = 0$; this means the bat is being treated as a perfectly rigid club. The dashed line shows a bat whose only elastic mode is #3, the simple bend. Note that this curve coincides with the rigid club model for an impact at the #3 node. To either side of this point, the bat can respond elastically, being somewhat more "mushy" in collision, and we see that the ball speed is correspondingly reduced. Hit at the node, the elastic bend can not be excited, and so the bat is equivalent to a rigid structure. Adair has exhibited a curve similar to this one based on an energy argument.[4]

The solid line in Fig. 6 shows the complete calculation using 20 elastic modes. The contribution of mode 20 to a is less than 0.1% relative to the total. The frequency of mode #5 is, as we see from the table, over 900 Hz, and the remaining 15 are of course even higher. This means that these higher modes can and do reverse their velocity at the impact point while the ball is still in contact.

The effect of higher modes on the effectiveness of the bat is readily apparent from the figure. The "sweet spot," defined as the maximum ball speed point, is slightly shifted relative to the other "sweet spots,"[5] the center of percussion—COP—at 68 cm and the #3 node at 69 cm. The maximum ball speed is increased even over the rigid club model, albeit by less than 1%.

The major effect occurs for a ball hit inside of the sweet spot. For a collision only 10 cm more proximal than optimum, the #3 mode would degrade the flight speed by 5% relative to the rigid club. In a vacuum model of the ball trajectory, this small difference costs 10%, or 42 ft of travel. (The ball velocity, again *in vacuo*, yields a 420-ft hit.) Given air resistance, that would not be over the center field wall. In any event, this sagging of the velocity curve would mean 40 ft shallower that the outfielder could stand and 40 ft less he would have to throw in order to hold the runners

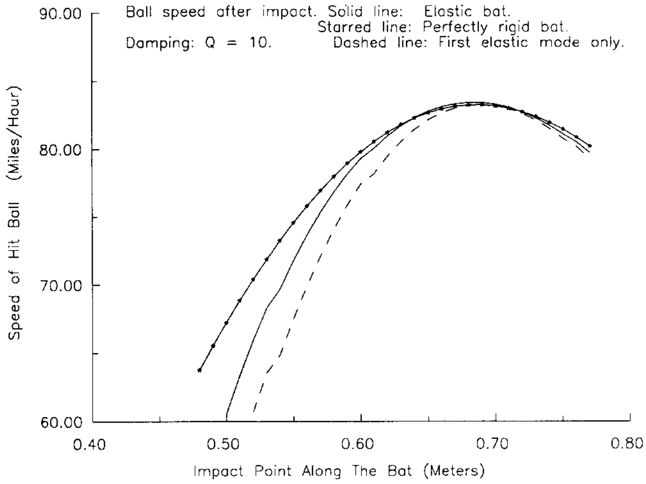

Fig. 6. The flight of the ball. The final ball recoil velocity is shown as a function of impact point along the length of the bat. In this graph, the ball crosses the plate with a speed of 40 m/s, and the bat meets it squarely with a center-of-mass speed of 16 m/s and an angular velocity of 34 rad/s. The parameters reflect major league but not superhuman performance. At the peak of the curve, the ball would travel 460 ft in a vacuum if the angle of elevation were an optimal 45°. The solid curve shows the performance to be expected from the elastic, wooden bat described in the text. The dashed curve shows the effect of suppressing all modes above #3, simple bending. The starred curve shows the performance expected for an infinitely rigid club having otherwise identical properties.

after a catch. In baseball, a game of very narrow margins, small does not mean insignificant. The other elastic modes restore about half of this degradation, hence they represent an important part of the bat performance factor.

Finally, the shape of Fig. 6 shows quantitatively how important to the batter it is to strike the ball with the outer end of the bat. As measured from the center of percussion, the ball speed is considerably more forgiving for hits to the outside than to the inside; mentioned before was the danger to the pitcher in giving the batter a good outside pitch.

Aluminum bats have all-around higher stiffness and correspondingly higher normal mode frequencies. All other things being equal, this effect alone would give aluminum bats a substantial edge over ash for the hitter, fully justifying their exclusion from the major leagues. All other things are not equal, however, and the aluminum bat needs a separate calculation of its own to be correctly compared to its wooden competition. (Ball velocity is probably not the reason for excluding aluminum from the majors. Rather the real reason seems to be the *failure* of aluminum to break on hitting an inside pitch.[6])

VII. CONCLUSIONS

We have seen that the theory of elasticity presented gives a comprehensive description of the performance of a wooden bat. The elastic normal modes contribute significantly to the range of the flight of the ball, both negatively and positively, depending on how the ball is hit. While we have not fully explored the question here, the normal modes can be strongly influenced by relatively minor changes in the cross-sectional contours of the bat. Since the normal mode frequencies can be readily measured, it is possible to imagine tuning the bat to produce optimum hitting performance. We have not, however, considered how shifts in the center of mass would influence the ability of the batter to accelerate the bat to maximum velocity. Nor have we considered the optimum mix of linear and rotational motion for which the batter should strive. (It is likely that 100 + years of empiricism in the game have already produced a shape close to the optimum.)

We have seen an indication of why the batting characteristics of a metal bat may be superior to wood, but this topic also was not fully explored.

We have seen why bats break on the catcher's side. We have also shown that the hitting performance is independent of boundary conditions on the handle, and may be safely studied using the free bat model.

Finally, we have displayed an interesting application of elasticity and normal mode theory to a familiar object and had considerable fun in doing so. And that, after all, is the central purpose of baseball, and among the professionals, of physics as well.

VIII. ADDED NOTE

After submission of this manuscript, the author visited the laboratory of Uwe Hansen at Indiana State University, and the bat in question was brought along. Professor Hansen performed a harmonic analysis of the bat modes, measuring eight frequencies spanning the range of his apparatus. If the handbook value for Young's modulus used above is increased by 35% to 1.62×10^{10} N/m^2 and the shear modulus is increased by almost as much to 1.05×10^{9} N/m^2, the theoretical frequencies and the measured frequencies match to the precision of the measurement. Specifically, see Table II.

The curve of frequency versus mode number departs substantially from the parabola predicted by the theory of a uniform bar.[2] That the theory follows this deviation as well as it does suggests that it is handling the nonuniform cross section well. The adjustments to the shear modulus change the higher frequencies by about 10–15 Hz, the low frequencies by 1 Hz or less. This difference reflects the increasing amount of shearing motion in the higher eigenvectors. As mentioned in the Introduction, the shear is dropped entirely from the conventional, analytic theory of the vibrating bar.

R. Adair, reading this manuscript before publication, has objected to some of the parameter values. Referring to his book,[4] Fig. 4.6, he feels the contact time should be re-

Table II. Theoretical frequencies and the measured frequencies matched to the precision of the measurement.

n	Theoretical	Experimental in Hz
3	171.5	170
4	562.2	560
5	1087.5	1100
6	1709.8	1720
7	2398.8	2410
8	3128.7	3130
9	3883.8	3880
10	4651.1	4630

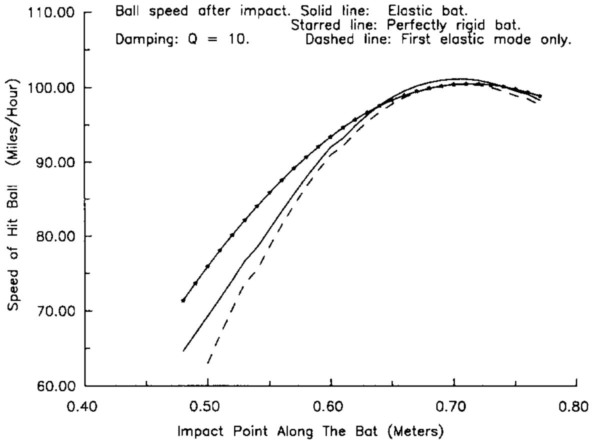

Fig. 7. Performance curve as in Fig. 6, but with modified parameters: contact time = 0.0006 s, bat COM velocity = 24 m/s, bat rotational speed = 51 /s, COR = 0.456. See Sec. VIII.

duced to 0.0006 s. He also argues for a smaller coefficient of restitution, and higher bat speed parameters. To investigate these matters, we increased the bat speed parameters by 50% (increasing the bat energy by over 100%), dropped the COR to 0.456, and cut the contact time to 0.0006 s. Figure 7 shows the results of these parameter changes. The higher frequency modes have become slightly less effective at giving back what the bending mode takes away on an inside hit but slightly more useful in the region near the sweet spots, and the top speed is increased to 102 mph at maximum.

ACKNOWLEDGMENTS

Dr. W. K. Schroll has graciously assisted in the preparation of Figs. 1 and 2. The author gratefully acknowledges the loan of the herein described wooden bat from Karl S. Van Zandt, who made no secret of his initial reservations at yielding it up for the performance of "experiments." I am also pleased to mention a most interesting colloquium by Professor R. Adair, which served as a stimulus to this work.

[1] H. Brody, "Models of Baseball Bats," Am. J. Phys. **58**, 756–758 (1990).

[2] P. M. Morse, *Vibration and Sound* (McGraw-Hill, New York, 1948), p. 156.

[3] S. Plagenhoef, *Patterns of Human Motion* (Prentice-Hall, Englewood Cliffs, NJ, 1971), p. 71.

[4] R. Adair, *The Physics of Baseball* (Harper & Row, New York, 1990), p. 89.

[5] H. Brody, "The Sweet Spot of a Baseball Bat," Am. J. Phys. **54**, 640–643 (1986).

[6] G. F. Will, *Men at Work: The Craft of Baseball* (MacMillan, New York, 1990), p. 124.

THE DANGERS OF STUDYING STATISTICAL MECHANICS

Ludwig Boltzmann, who spent much of his life studying statistical mechanics, died in 1906, by his own hand. Paul Ehrenfest, carrying on the work, died similarly in 1933. Now it is our turn to study statistical mechanics. Perhaps it will be wise to approach the subject cautiously.

David L. Goodstein, *States of Matter* (Prentice-Hall, Englewood Cliffs, NJ, 1975; reprinted by Dover, Mineola, NY, 1985).